J Physiol 599.15 (2021) pp 3715–3733

The Journal of Physiology

Impaired skeletal muscle fatigue resistance during cardiac hypertrophy is prevented by functional overload- or exercise-induced functional capillarity

Peter G. Tickle[1], Paul W. Hendrickse[2,3], Andrew Weightman[4], M. Hakam Nazir[1], Hans Degens[2,3] and Stuart Egginton[1]

[1]*School of Biomedical Sciences, University of Leeds, Leeds, UK*
[2]*Department of Life Sciences, Research Centre for Musculoskeletal Science & Sports Medicine, Manchester Metropolitan University, Manchester, UK*
[3]*Institute of Sport Science and Innovations, Lithuanian Sports University, Kaunas, Lithuania*
[4]*Department of Mechanical, Aerospace and Civil Engineering, University of Manchester, Manchester, UK*

Edited by: Michael Hogan & Caroline Rickards

The peer review history is available in the Supporting Information section of this article (https://doi.org/10.1113/JP281377#support-information-section).

Key points

- Capillary rarefaction is hypothesized to contribute to impaired exercise tolerance in cardiovascular disease, but it remains a poorly exploited therapeutic target for improving skeletal muscle performance.
- Using an abdominal aortic coarctation rat model of compensatory cardiac hypertrophy, we determine the efficacy of aerobic exercise for the prevention of, and mechanical overload for, restoration of hindlimb muscle fatigue resistance and microvascular impairment in the early stages of heart disease.
- Impaired muscle fatigue resistance was found after development of cardiac hypertrophy, but this impairment was prevented by low-intensity aerobic exercise and recovered after mechanical stretch due to muscle overload.
- Changes in muscle fatigue resistance were closely related to functional (i.e. perfused) microvascular density, independent of arterial blood flow, emphasizing the critical importance of optimal capillary diffusion for skeletal muscle function.
- Pro-angiogenic therapies are an important tool for improving skeletal muscle function in the incipient stages of heart disease.

Peter G. Tickle is working on aspects of skeletal muscle physiology and biomechanics as a postdoctoral researcher at the University of Leeds. He is particularly interested in the underlying factors that regulate muscle performance such as muscle blood flow, the microcirculation, energy consumption and the influence of disease. His current work is focused on characterizing the mechanics of very high frequency insect flight muscle contractions using the work loop technique with Dr Graham Askew. **Paul W. Hendrickse** received his PhD from Manchester Metropolitan University for his research into the role of the microcirculation in skeletal muscle function and plasticity. He currently works as a postdoctoral research associate under the direction of Professor Hans Degens, studying the effect of countermeasures to unloading in bed rest on muscle morphology.

Peter G. Tickle and Paul W. Hendrickse contributed equally to this study.

DOI: 10.1113/JP281377

Abstract Microvascular rarefaction may contribute to declining skeletal muscle performance in cardiac and vascular diseases. It remains uncertain to what extent microvascular rarefaction occurs in the earliest stages of these conditions, if impaired blood flow is an aggravating factor and whether angiogenesis restores muscle performance. To investigate this, the effects of aerobic exercise (voluntary wheel running) and functional muscle overload on the performance, femoral blood flow (FBF) and microvascular perfusion of the extensor digitorum longus (EDL) were determined in a chronic rat model of compensatory cardiac hypertrophy (CCH, induced by surgically imposed abdominal aortic coarctation). CCH was associated with hypertension ($P = 0.001$ *vs.* Control) and increased relative heart mass ($P < 0.001$). Immediately upon placing the aortic band (i.e. before development of CCH), post-fatigue test FBF was reduced ($P < 0.003$), coinciding with attenuated fatigue resistance ($P = 0.039$) indicating an acute arterial perfusion constraint on muscle performance. While FBF was normalized during CCH in chronic groups ($P > 0.05$) fatigue resistance remained reduced ($P = 0.039$) and was associated with reduced ($P = 0.009$) functional capillarity after development of CCH without intervention, indicating a microvascular limitation to muscle performance. Normalization of functional capillarity after aerobic exercise ($P = 0.065$) and overload ($P = 0.329$) in CCH coincided with restoration to control levels of muscle fatigue resistance ($P > 0.999$), although overload-induced EDL hypertrophy ($P = 0.027$) and wheel-running velocity and duration (both $P < 0.05$) were attenuated after aortic banding. These data show that reductions in skeletal muscle performance during CCH can be countered by improving functional capillarity, providing a therapeutic target to improve skeletal muscle function in chronic diseases.

(Received 16 January 2021; accepted after revision 4 June 2021; first published online 9 June 2021)
Corresponding author Prof. S. Egginton: School of Biomedical Sciences, Faculty of Biological Sciences, University of Leeds, Leeds LS2 9JT, UK. Email: s.egginton@leeds.ac.uk

Introduction

Persistent exercise intolerance is a hallmark of chronic heart failure (CHF), compromising quality of life and contributing to a poor clinical prognosis. Skeletal muscle performance is, however, poorly correlated with left ventricular ejection fraction in CHF (Franciosa *et al.* 1981; Rogers, 2001), suggesting that peripheral factors determine the severity of exercise intolerance (Pandey *et al.* 2015). Further pathological changes in CHF contributing to impaired exercise performance include sarcopenia and a slow-to-fast change in muscle fibre type composition (Drexler *et al.* 1992). In addition, there is growing evidence for constraints imposed by structural and functional changes in the microcirculation in the muscle (Duscha *et al.* 1999; Richardson *et al.* 2003; Tickle *et al.* 2020). Reduced skeletal muscle microvascular density occurs in both experimentally induced (Kindig *et al.* 1999; Nusz *et al.* 2003; Richardson *et al.* 2003; Bowen *et al.* 2017) and clinical (Schaufelberger *et al.* 1995; Duscha *et al.* 1999; Wadowski *et al.* 2018) CHF, and this rarefaction imposes a limit on the transfer of oxygen and nutrients, and removal of waste products, to and from respiring muscle tissue. Indeed, there is strong evidence for a key role of the *perfused* microcirculation in determining performance of cardiac (Hauton *et al.* 2015) and skeletal muscle (Tickle *et al.* 2020). The perfused, or functional, microcirculation is expected to be equivalent to the total, or anatomical, microcirculation in healthy tissue, whereby every vessel is available for blood flow. Experimentally induced arteriolar blockade to simulate the early stages of functional rarefaction indicates that muscle performance is strongly associated with the degree of perfused vessels, regardless of total underlying capillarity (Tickle *et al.* 2020). Skeletal muscle capillary rarefaction after imposition of cardiac dysfunction indicates that systemic effects may occur soon (<21 days) after development of perturbed heart function (Nusz *et al.* 2003), potentially due to enhanced endothelial apoptosis (Rossig *et al.* 2000) or increased vasoconstriction leading to arteriolar closure (Prewitt *et al.* 1982). Coupled to the deleterious effects of rarefaction, a disturbed anatomical distribution of capillaries may also compromise muscle function because increased heterogeneity of capillary spacing can reduce tissue oxygenation (Piiper & Scheid, 1991; Degens *et al.* 2006b). Furthermore, animal models of CHF demonstrate reduced red blood cell velocity and flux (Richardson *et al.* 2003), in addition to an increased proportion of capillaries with intermittent RBC flux at rest and during contractile activity (Kindig *et al.* 1999). The consequent increase in transit time potentially explains the higher oxygen extraction observed in CHF (Katz *et al.* 2000), but also suggests that muscle oxygenation is impaired, leading to suboptimal mitochondrial function (Behnke *et al.* 2007).

Improving muscle and exercise performance in CHF may therefore depend upon restoration of optimal topology of the microcirculation. However, it remains unknown whether capillary distribution and/or capillary perfusion is changed during CHF, and whether these putative changes affect skeletal muscle oxygenation, performance and capacity for adaptive remodelling.

Capillary proliferation from pre-existing vessels (angiogenesis) in skeletal muscle is an essential adaptation to match tissue performance to changing functional demands (Brodal *et al.* 1977; Zumstein *et al.* 1983) that is triggered by both physical and metabolic stimuli (Hudlicka, 1991). For example, the increased longitudinal strain on the abluminal capillary surface (Egginton *et al.* 2001) during functional overload of a muscle (via extirpation of a muscle synergist, hereafter 'overload') not only results in hypertrophy (Zhou *et al.* 1998; Deveci & Egginton, 2002; Tickle *et al.* 2020) and enhanced fatigue resistance (i.e. slower rate of active force decline) (Frischknecht & Vrbova, 1991; Ballak *et al.* 2016; Tickle *et al.* 2020), but also induces angiogenesis (Egginton *et al.* 1998, 2011; Williams *et al.* 2006; Ballak *et al.* 2016). The significance of angiogenesis for function is illustrated by the observation that even after experimentally induced functional capillary rarefaction, overload-mediated angiogenesis can recover capillarization and fatigue resistance in otherwise healthy muscle (Tickle *et al.* 2020).

In addition to the pro-angiogenic effects of longitudinal strain, capillary proliferation can be induced by enhanced vascular shear stress via application of a hyperaemic stimulus such as occurs during chronic electrical stimulation of muscle (Hudlicka *et al.* 1977; Egginton & Hudlicka, 1999) or vasodilator administration (Egginton *et al.* 2016; Mandel *et al.* 2016). While the hyperaemic stimulus undoubtedly contributes to expansion of the microvascular bed (Waters *et al.* 2004; Olesen *et al.* 2010) with prolonged aerobic exercise training (Andersen & Henriksson, 1977), exercise-induced angiogenesis is also mediated by metabolic (e.g. hypoxia, glucose metabolism) factors (Olfert *et al.* 2016). In clinical (Gustafsson *et al.* 2001; Esposito *et al.* 2010, 2018) and experimental (Ranjbar *et al.* 2017) CHF, enhanced capillarity and angiogenic signalling (e.g. via vascular endothelial growth factor, VEGF) are found after exercise therapy, indicating that the capacity for remodelling is still present despite established disease. Improvements in peak oxygen consumption after exercise therapy in CHF patients are also considered to be driven by improvements in peripheral microvascular function (Haykowsky *et al.* 2012). In CHF patients without exercise therapy, contradictory data on angiogenic marker expression have been reported. For instance, elevated VEGF (Valgimigli *et al.* 2004) is hypothesized to drive repair of endothelial damage rather than expanding microvascular density *per se* (Chong *et al.* 2004). In another study, however, reduced VEGF expression (Arakawa *et al.* 2003) was indicative of regulatory dysfunction and the potential of multiple factors (e.g. severity and specific type of CHF) to affect capillary proliferation in muscle tissue. Nevertheless, the beneficial effects of exercise-induced angiogenesis for restoring muscle function suggest that intrinsic remodelling capacity may be harnessed, but this remains a poorly exploited therapeutic target.

The principal objective of this paper was therefore to quantify the functional and structural effects of angiogenic stimuli on skeletal muscle during compensatory cardiac hypertrophy (CCH) induced by coarctation of the abdominal aorta (Degens *et al.* 2006a), a model of incipient cardiac dysfunction. We tested in this rat model the following specific hypotheses: (1) CCH has a deleterious effect on skeletal muscle microcirculation and fatigue resistance; (2) exercise prevents the adverse effects of CCH on skeletal muscle; (3) overload has a restorative effect on impaired skeletal muscle capillarization and fatigue resistance in rats with CCH. By quantifying the effects of cardiac dysfunction on skeletal muscle function and microcirculation, we provide further evidence that the perfused microvascular bed is a therapeutic target for skeletal muscle dysfunction in chronic diseases such as CHF.

Methods

Ethical approval

All experimental work complied with the UK Animals (Scientific Procedures) Act 1986, and local approval (70/08674) was granted by the University of Leeds Animal Welfare and Ethical Review Committee. All experiments conformed to the principles and regulations described by guidelines published in the *Journal of Physiology* (Grundy, 2015).

Aortic constriction and EDL overload

Experiments were designed to enable comparison of the effects of aerobic exercise and/or functional overload on muscle morphology, performance and blood flow after establishment of CCH. In-house bred male Wistar rats were used throughout. While heart disease is not specific to either sex, male rats were used as an extensive body of complementary data is available, and constraints of time and funding precluded an expansion of the study. Compensatory cardiac hypertrophy was induced via abdominal aortic constriction using a titanium band ('banded' groups). Groups of aortic banded animals were allocated as follows: (i) banded control (Aob: 304 ± 6 g, $N = 7$); (ii) unilateral overload of the EDL (Aob+OV: 376 ± 6 g, $N = 7$); (iii) voluntary wheel running (Aob+EX: 305 ± 12 g, $N = 7$); (iv) acute banded, in which the

immediate effects of banding were quantified (Acute-Aob: 245 ± 40 g, $N = 6$). Corresponding non-banded groups were also used: (i) intact (Control: 257 ± 8 g; $N = 7$); (ii) overload (OV: 343 ± 9 g, $N = 7$); (iii) wheel running (EX: 316 ± 41 g, $N = 8$). Only EX and Aob+EX had access to a cage wheel, all other groups were sedentary. All groups had *ad libitum* access to food and water and were housed under a 12 h light/dark cycle.

Under isoflurane anaesthesia (induction 4%, maintenance 2.5%) rats underwent surgery to constrict the abdominal aorta immediately cranial to the renal artery bifurcations using a titanium clip (post-mortem measured clip diameter: 0.37 ± 0.07 mm Ligaclip; Ethicon Endo-Surgery Inc., Cincinnati, OH, USA) (Cornelussen *et al*. 1994; Levy *et al*. 1996; Degens *et al*. 2006a). Depth of anaesthesia was regularly assessed by testing the pedal withdrawal reflex. Aob and Aob+EX were otherwise intact. Unilateral mechanical overload of the extensor digitorum longus (EDL) (Zhou *et al*. 1998; Deveci & Egginton, 2002; Tickle *et al*. 2020) was performed in Aob+OV 4 weeks after clip placement. In this procedure, extirpation of the tibialis anterior induces stretch and functional overload of the EDL. Post-operative analgesia (buprenorphine (Vetergesic, Ceva, Amersham, UK) 0.05 mg kg^{-1}) and antibiotic (Enrofloxacin (Baytril, Bayer, Reading, UK) 2.5 mg kg^{-1}) were provided after all surgical procedures. Muscle fatigue resistance and hindlimb perfusion in Aob and Aob+EX was quantified 4 weeks after aortic constriction, and in Aob+OV after an additional 2 weeks.

The overload model of muscle angiogenesis was selected because the success, or lack thereof, depends upon weight-bearing and voluntary activity; actions that may be easily translated to the clinical setting. In contrast, other effective angiogenic stimuli such as imposition of a clean stretch or elevated shear stress (e.g. via electrical stimulation or α_1-blocker administration) were considered less suitable in this context because they either require unwieldy treatment (e.g. fixing muscle length for long periods by limb immobilization (Goldspink *et al*. 1995)), potentially incur pharmaceutical side-effects, may drive angiogenesis without corresponding functional benefit (Kissane *et al*. 2021), and/or may compound CHF-derived hypotension via vascular dilatation.

Wheel running

EX and Aob+EX animals were housed in a cage with *ad libitum* access to an instrumented running wheel that enabled real-time monitoring of night-time exercise performance (distance moved, exercise duration and running speed) via bespoke LabVIEW software ('Rodent voluntary exercise analysis system' developed in conjunction with the University of Manchester, UK). Access to the wheel was provided immediately after aortic constriction surgery for Aob+EX. To ensure access to the running wheel was the same for each animal and exclude erroneous data due to disturbance, all cage wheels were locked during weekly cage cleaning and welfare checks.

Muscle fatigue resistance and hindlimb perfusion

Protocols for measuring muscle fatigue resistance and arterial blood flow are described in Tickle *et al* (2020). In brief, anaesthesia was induced with isoflurane (4% in 100% O_2) and thereafter maintained by constant alfaxalone (Jurox, Crawley, UK) infusion (30–35 mg kg hr^{-1}) delivered via a catheter in the external jugular vein. Implanted carotid and tail artery catheters allowed continuous measurement (blood pressure transducer: AD Instruments, UK) of central and peripheral blood pressure, and heart rate. Adequate depth of surgical anaesthesia was regularly assessed by reference to heart rate and blood pressure in addition to tests of the pedal withdrawal reflex.

Bilateral EDL isometric twitch force at optimal length was measured by linking each muscle to a lever arm force transducer (305B-LR: Aurora Scientific, Aurora, ON, Canada) and providing supramaximal electrical stimulation via the popliteal nerve (Hudlicka *et al*. 1977). Unimpeded access to the EDL was facilitated by extirpation of the overlying synergist tibialis anterior. To determine EDL fatigue resistance, a 30 s period of 1 Hz twitches, to activate the metabolic machinery, was followed by 10 Hz impulses (0.3 ms pulse width, supra-maximal voltage) for 180 s (Egginton & Hudlicka, 1999; Tickle *et al*. 2020). No evidence of muscle ischaemia (rapid decline in twitch force, slowing of twitch time course) was noted during experiments, indicating that the stimulation protocol did not constrain muscle blood flow via increased intra-muscular pressure. Fatigue resistance was quantified as a 'fatigue index' (FI) that was calculated as muscle force at the end of the test divided by peak muscle tension at the beginning of the test. A mean of five consecutive twitches was selected to represent end-stimulation and peak force data.

The femoral artery blood flow (FBF) was measured bilaterally throughout each experiment with perivascular flow probes (0.7PSB; Transonic, Ithaca, NY, USA) at the proximal aspect of the *profunda femoris* arterial bifurcation (Tickle *et al*. 2020). The muscle mass-specific increase in flow, i.e. hyperaemic increment above resting, was calculated to account for potential differences in EDL mass and transformed to femoral vascular conductance using arterial pressure measured in the tail. While measured continuously, for clarity we present blood flow at rest and immediately post-stimulation (when peak blood flow was typically evident).

Following the conclusion of each experiment, capillary perfusion was visualized by an injection of fluorescein

isothiocyanate (FITC) – labelled dextran solution (50 mg kg^{-1}, MW = 500,000; Sigma, Poole, UK) via the carotid artery (Tickle *et al.* 2020). Before and after injection, the EDL in both legs were stimulated at 4 Hz for 30 s to induce functional hyperaemia and capillary recruitment. EDL were left *in situ* for a minimum of 1 min after injection to maximize dye localization in perfused capillaries (Snyder *et al.* 1985). While still under general anaesthesia, animals were then killed by cervical dislocation.

Histology

Immediately after animals were killed, the EDL muscles were removed, blotted dry and weighed. The muscle was then frozen on cork with OCT embedding medium (Thermo Scientific, Loughborough, UK) using liquid nitrogen-cooled isopentane and stored at −80°C. Ten-micrometre cryostat sections were prepared and labelled with biotinylated *Griffonia simplicifolia* lectin I (5 μl ml^{-1} FL-1101 GSL I; Vector Labs, Peterborough, UK) and streptavidin Alexa Fluor 350 conjugate. For fibre typing, serial sections were blocked in 10% goat serum in PBS for 60 min (Vector Laboratories, USA) then incubated for 120 min with monoclonal antibodies BAD-5 (1:600), SC-71 (1:600), 6H1 (1:50) on one slide and BF-F3 (1:100) on another in blocking solution for fibre types I, IIa, IIx and IIb, respectively (Developmental Studies Hybridoma Bank, USA). After three 5 min washes in PBS the sections were incubated in the dark with secondary antibodies Alexa Fluor IgG2b for type I (1:500), Alexa Fluor IgG1 for type IIa (1:500) and Alexa Fluor 555 IgM for types IIb and IIx (1:500) (Thermofisher Scientific, USA) in blocking solution. After three further 5 min washes the slides were mounted with ProLong Diamond Antifade mountant (Thermofisher Scientific, USA). Whole-muscle cross-sectional images were acquired with a confocal microscope (Leica TCS SP5) at ×20 magnification. Subsequent image analysis with BTablet and Anatis (BaLoH Software, Ooij, The Netherlands) enabled determination of fibre type, fibre cross-sectional area and whether capillaries were perfused (i.e. FITC labelled). To account for the regional heterogeneity of capillary distribution and fibre-type composition (Kissane *et al.* 2018) three regions of interest (475 × 475 μm^2) of the whole-muscle image were used to establish an unbiased counting frame with which to quantify muscle fibre type composition (numerical fibre type proportions and the specific fibre cross-sectional area, FCSA), capillarization (expressed as capillary to fibre ratio, C:F, or capillary density, CD) and capillary domain area (CDA). CDA quantifies the area surrounding a capillary defined by equidistant boundaries from adjacent capillaries and is an index of the area of tissue to which a capillary may supply adequate oxygen to working muscle (Hoofd *et al.* 1985; Al-Shammari *et al.* 2014). Heterogeneity of capillary distribution is provided by Log_{RSD}. Capillary localization was completed as described in Tickle *et al.* (2020). Sample sizes for histological parameters were reduced in EX ($N = 5$) and OV ($N = 5$) due to tissue damage.

Mathematical modelling of tissue PO_2 distribution was performed in representative ($N = 1$ in each group) EDL histological sections using a custom MATLAB program ('Oxygen Transport Modeler') (Al-Shammari *et al.* 2019). Model input assumptions include capillary radius, muscle oxygen demand, myoglobin concentration, oxygen solubility and diffusivity; and since measurements of these parameters were not possible in this study, values were applied uniformly across groups (Tickle *et al.* 2020). Therefore, while the absolute values produced by this model should be interpreted with caution, the calculated tissue PO_2 serves as an indicative comparison of the effects of functional capillary rarefaction between groups.

Statistical analyses

In all cases, differences in FI, blood flow and histological parameters between groups were quantified using ANOVA with Tukey's *post hoc* tests. ANCOVA with Sidak's *post hoc* tests were used to test whether aortic banding influenced heart mass after controlling for the scaling effect of body mass (Solomon & Bengele, 1973). Statistical testing was conducted in SPSS (v.25). Data are presented throughout as means ± SD unless stated otherwise and statistical tests were considered significant where $P < 0.05$.

Results

Cardiovascular effects of aortic banding

Acute-Aob had an mean arterial (carotid) pressure that did not significantly differ from any group, while tail pressure was lower than all other groups ($P < 0.002$), thereby producing a greater carotid:tail BP ratio (Table 1; $P < 0.001$). Carotid pressure was higher after chronic banding compared with all unbanded groups (Fig. 1; Con *vs.* Aob: $P = 0.001$; EX *vs.* Aob+EX: $P = 0.026$; OV *vs.* Aob+OV: $P = 0.031$). Tail blood pressure was higher in EX ($P = 0.039$) and Aob+EX ($P = 0.016$) than Control (Table 1). There were no significant differences in heart rate between groups.

Relative heart mass was lower in Control and OV animals than in exercised (Con: $P = 0.028$; OV: $P = 0.046$) and banded animals (Con *vs.* Aob: $P < 0.001$; *vs.* Aob+EX: $P < 0.001$; *vs.* Aob+OV: $P = 0.001$; OV *vs.* Aob, Aob+EX & Aob+OV: $P < 0.001$); the cardiac enlargement in EX (compared with Control: $P = 0.028$) was smaller than the compensatory hypertrophy in Aob ($P = 0.005$) but similar

Table 1. Cardiovascular response to aortic banding

	Control	EX	OV	Acute-Aob	Aob	Aob + EX	Aob + OV
Body mass (g)	254 ± 44^{ab}	316 ± 41^{c}	343 ± 23^{cd}	245 ± 40^{a}	304 ± 17^{bc}	305 ± 33^{bc}	375 ± 17^{d}
Heart mass (% M_b)	0.27 ± 0.04^{a}	0.32 ± 0.04^{b}	0.26 ± 0.04^{a}	-	0.38 ± 0.04^{c}	0.35 ± 0.04^{bc}	0.35 ± 0.04^{bc}
MAP (carotid) (mmHg)	122 ± 3^{a}	124 ± 13^{a}	123 ± 8^{a}	139 ± 12^{ab}	157 ± 25^{b}	148 ± 14^{b}	147 ± 11^{b}
MAP (tail) (mmHg)	92 ± 7^{ab}	115 ± 11^{c}	92 ± 13^{a}	58 ± 16^{d}	115 ± 21^{bc}	119 ± 12^{c}	96 ± 15^{abc}
Carotid:tail MAP ratio	1.33 ± 0.13^{a}	1.08 ± 0.11^{a}	1.36 ± 0.22^{a}	2.54 ± 0.73^{b}	1.39 ± 0.22^{a}	1.25 ± 0.14^{a}	1.55 ± 0.23^{a}
Heart rate (bpm)	394 ± 43^{a}	383 ± 53^{a}	347 ± 48^{a}	356 ± 68^{a}	359 ± 59^{a}	400 ± 43^{a}	397 ± 31^{a}

Abbreviations: M_b, body mass; MAP, mean arterial pressure. Statistically significant differences between groups across each row are denoted by letters; groups sharing the same letter were not different, those with no shared letters were statistically different ($P < 0.05$) as determined by ANOVA with Tukey's *post hoc* tests.

to Aob + EX ($P = 0.904$) and Aob + OV ($P > 0.939$); there was no difference between banded groups' heart mass (Aob *vs.* Aob+EX: $P = 0.349$; Aob *vs.* Aob+OV: $P = 0.632$; Aob+EX *vs.* Aob+OV: $P = 0.999$).

Wheel running

The velocity (week (wk) 1: $P = 0.024$; wks 2, 3 & 4: $P < 0.001$) and duration (wk 1: $P = 0.014$; wk 2, 3 & 4: $P < 0.001$) of each exercise bout, and therefore total distance travelled (wk 1: $P = 0.001$; wk 2, 3 & 4: $P < 0.001$), were significantly lower in Aob+EX than in EX, while motivation to exercise (number of bouts) was otherwise undiminished after band application (wk 1: $P = 0.128$; wk 2: $P = 0.419$; wk 3: $P = 0.750$; wk 4: $P = 0.733$), indicating a constraint on voluntary exercise stamina imposed by CCH (Fig. 2, Table 1).

Muscle performance

The FI was impaired compared with Control immediately after band application (Acute-Aob ($P < 0.001$)) and remained impaired after 4 weeks ($P = 0.039$; Fig. 3, Table 2). The FI was comparable to Control in Aob+EX ($P = 0.999$) and Aob+OV ($P = 0.999$) and was significantly higher than Aob ($P = 0.039$) While overload improved FI in OV ($P = 0.036$), FI in EX was similar to Control ($P = 0.954$).

Femoral artery perfusion

Resting femoral artery flow (ml·min^{-1}) was significantly lower in Acute-Aob compared with all other groups (*vs.* Control: $P = 0.003$; *vs.* OV: $P = 0.036$; *vs.* all others: $P < 0.001$), Fig. 4*A*). End-stimulation FBF was

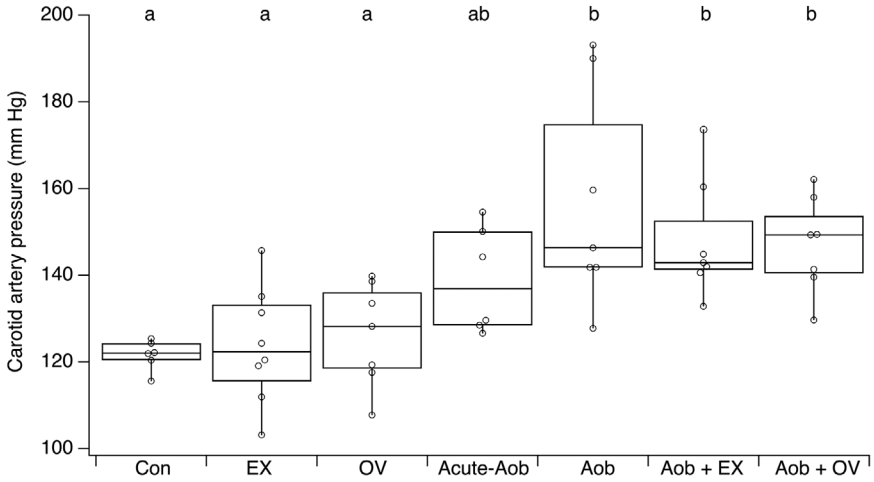

Figure 1. Hypertension after chronic abdominal aortic stenosis
Chronic restriction of blood flow via the abdominal aorta caused an increased mean carotid artery pressure at 4 weeks (aortic banded (Aob): $N = 7$; $P = 0.001$; aortic banded with exercise intervention (Aob + EX): $N = 7$; $P = 0.018$) and 6 weeks (aortic banded with muscle overload (Aob + OV): $N = 7$; $P = 0.027$). An intermediate blood pressure between unbanded (Control ($N = 7$); EX ($N = 8$); OV ($N = 7$) and banded animals was evident during the acute phase after band application (Acute-Aob; $N = 6$). Statistically significant differences between groups are denoted by letters; groups sharing the same letter were not different, those sharing none were statistically different ($P < 0.05$) as determined by ANOVA with Tukey's *post hoc* tests.

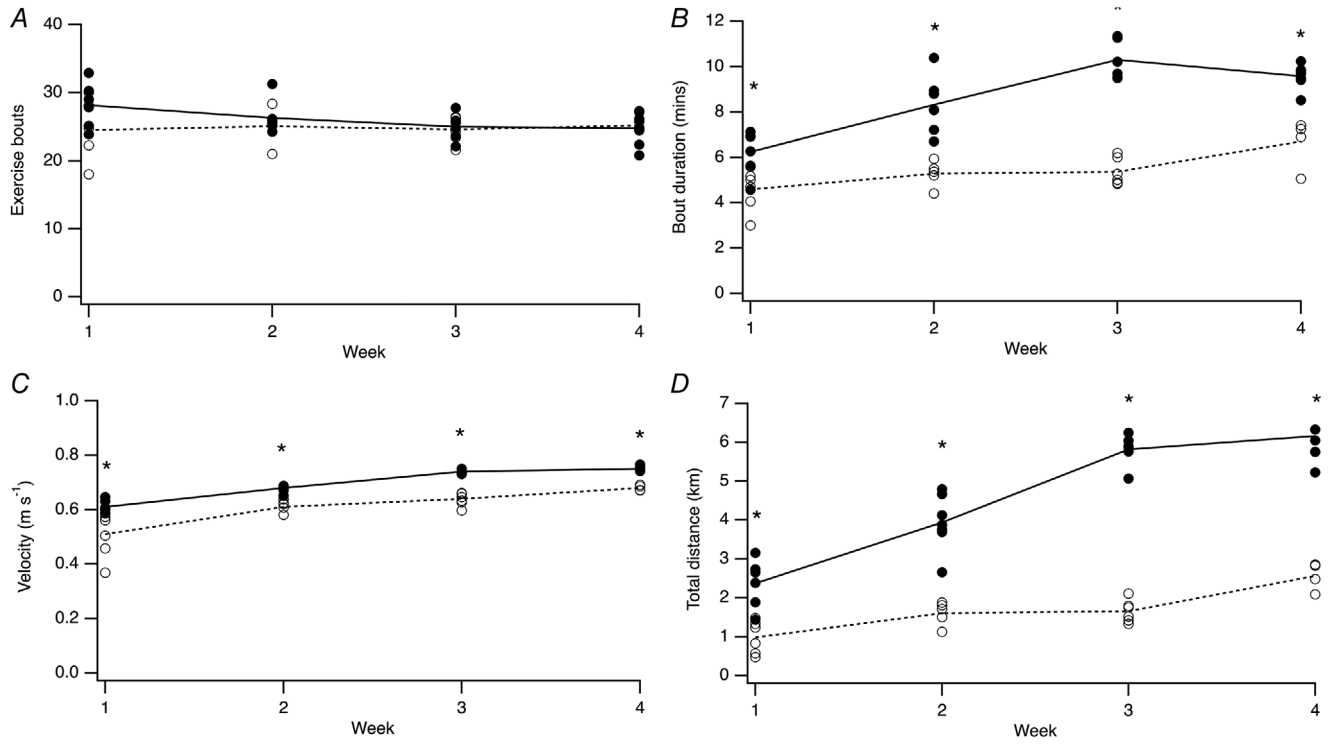

Figure 2. Impaired voluntary wheel-running exercise performance after abdominal aortic banding
While inclination to exercise was undiminished (*A*), bout duration (*B*), velocity (*C*) and total distance travelled (*D*) were reduced in banded animals (Aob+EX: dashed line) compared with exercise controls (EX: continuous line). Interpolation lines fitted through the mean at each timepoint for each group. Asterisks denote statistical significance between EX ($N = 8$) and Aob+EX ($N = 7$) at each timepoint ($P < 0.05$).

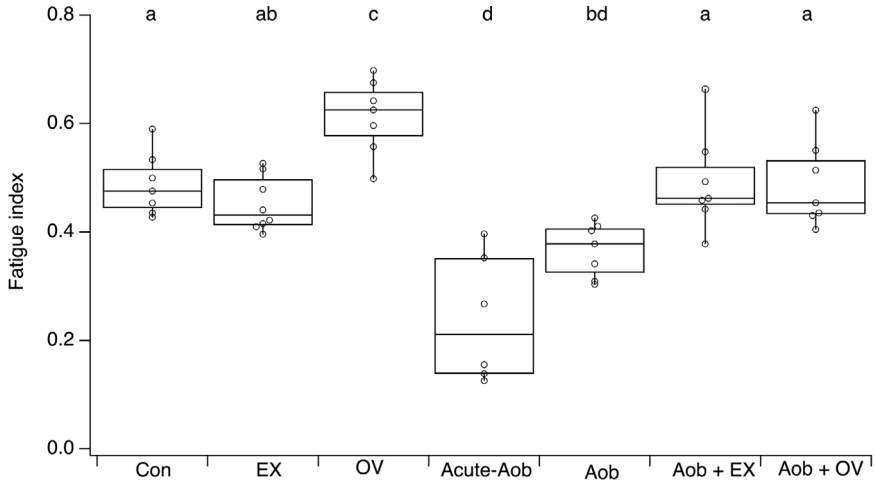

Figure 3. Impaired muscle fatigue resistance accompanied compensatory cardiac hypertrophy but recovered after intervention
Fatigue index (FI) was reduced immediately after band application and remained impaired for 4 weeks without intervention (Aob: $P = 0.039$). Exercise (Aob+EX) and overload (Aob+OV) recovered fatigue resistance to control levels (both $P = 0.999$) despite the chronic effects of aortic banding. Group sizes were the same as in Fig. 1. Statistically significant differences between groups are denoted by letters; groups sharing the same letter were not different, those sharing none were statistically different ($P < 0.05$) as determined by ANOVA with Tukey's *post hoc* tests.

Table 2. EDL fatigue resistance, isometric twitch performance and hindlimb blood flow

	Control	EX	OV	Acute-Aob	Aob	Aob + EX	Aob + OV
Fatigue index	0.49 ± 0.06[a]	0.45 ± 0.05[ab]	0.61 ± 0.07[c]	0.27 ± 0.10[d]	0.37 ± 0.05[bd]	0.49 ± 0.09[a]	0.49 ± 0.08[a]
Maximum twitch tension (N)	0.32 ± 0.09[a]	0.35 ± 0.17[a]	0.40 ± 0.18[ab]	0.26 ± 0.09[a]	0.31 ± 0.03[a]	0.29 ± 0.06[a]	0.54 ± 0.11[b]
Maximum twitch tension per g EDL (N/g)	2.25 ± 0.58[a]	1.80 ± 0.82[a]	1.85 ± 0.86[a]	2.17 ± 0.89[a]	1.83 ± 0.28[a]	1.71 ± 0.21[a]	2.32 ± 0.59[a]
Rise time 25–75% (ms)	7.2 ± 0.5[a]	6.7 ± 0.8[a]	7.1 ± 0.8[a]	6.8 ± 0.9[a]	6.5 ± 1.0[a]	6.7 ± 1.1[a]	5.8 ± 0.9[a]
Fall time 75–25% (ms)	19.4 ± 2.9[ab]	16.0 ± 5.0[a]	23.7 ± 6.9[b]	21.2 ± 3.1[ab]	14.8 ± 4.5[a]	17.3 ± 2.9[ab]	14.8 ± 3.0[a]
Femoral flow (ml/min)rest	1.09 ± 0.22[a]	1.32 ± 0.39[a]	0.97 ± 0.19[a]	0.48 ± 0.21[b]	1.23 ± 0.19[a]	1.39 ± 0.32[a]	1.27 ± 0.29[a]
End-stimulation	1.74 ± 0.23[ab]	2.07 ± 0.81[a]	1.92 ± 0.95[a]	0.96 ± 0.48[b]	1.80 ± 0.46[ab]	2.13 ± 0.42[a]	2.04 ± 0.50[a]
Hyperaemic scope (end-stimulation / rest)	1.62 ± 0.25[a]	1.61 ± 0.61[a]	1.96 ± 0.76[a]	1.95 + 0.59[a]	1.48 + 0.34[a]	1.60 ± 0.49[a]	1.62 ± 0.31[a]
Hyperaemic increase per g EDL (ml/min/g)	4.28 ± 1.47[a]	3.75 ± 3.62[a]	4.59 ± 4.09[a]	4.06 ± 2.65[a]	3.28 ± 2.42[a]	4.31 ± 1.82[a]	3.34 ± 1.76[a]
Hyperaemic increase FVC (ml/min/mmHg/g)	0.050 ± 0.018[a]	0.039 ± 0.035[a]	0.047 ± 0.045[a]	0.063 ± 0.04[a]	0.035 ± 0.033[a]	0.048 ± 0.030[a]	0.048 ± 0.015[a]

Abbreviations: EDL, extensor digitorum longus; FVC, femoral artery vascular conductance. Statistically significant differences between groups across each row are denoted by letters; groups sharing the same letter were not different, those with no shared letters were statistically different ($P < 0.05$) as determined by ANOVA with Tukey's *post hoc* tests.

lower in the Acute-Aob than EX ($P = 0.022$), Aob+EX ($P = 0.018$) and Aob+OV ($P = 0.037$) groups, but not significantly different from Control ($P = 0.255$), OV ($P = 0.081$) and Aob ($P = 0.177$) (Fig. 4*B*; Table 2). Hyperaemic scope was similar in all groups. The magnitude of hyperaemic flow per gramme of EDL did not differ significantly between groups, even when accounting for femoral vascular conductance per gramme of muscle tissue (FVC) (Table 2).

Muscle mass and histology

EDL mass as a proportion of body mass was increased in OV compared with Control ($P = 0.036$), Aob ($P = 0.023$) and Aob+EX ($P = 0.038$), but was similar to EX ($P = 0.544$) and Aob+OV ($P = 0.938$) (Table 3). The magnitude of muscle hypertrophy after overload was, however, greater in OV compared with Aob+OV ($P = 0.027$; Table 3).

Anatomical CD did not differ significantly between Control and any aortic banded animals (Aob: $P = 0.999$; Aob+EX: $P = 0.938$; Aob+OV: $P = 0.465$). OV had an increased anatomical CD compared with Control ($P = 0.029$), thereby indicating angiogenesis had occurred that exceeded the degree of fibre hypertrophy. Development of CCH precipitated a significant reduction in perfused CD in Aob ($P < 0.001$), Aob+EX ($P = 0.001$) and Aob+OV ($P < 0.001$) (compared with non-banded controls). Perfused CD was not significantly different between banded groups (Table 3).

While anatomical C:F was unchanged across groups compared with Control, it was increased in Aob+OV compared with Aob ($P = 0.028$) and Aob+EX ($P = 0.002$). Compared with unbanded groups, perfused C:F was reduced in Aob ($P = 0.009$). In contrast, perfused C:F was recovered in Aob+EX ($P = 0.065$) and Aob+OV ($P = 0.329$) and was not significantly different ($P < 0.05$) from Control (Table 3).

Compared with Control, anatomical CDA was increased in Aob ($P = 0.009$) while similar in Aob+EX ($P = 0.845$) and Aob+OV ($P = 0.999$) (Table 3). In contrast, a more pronounced effect was obvious in the

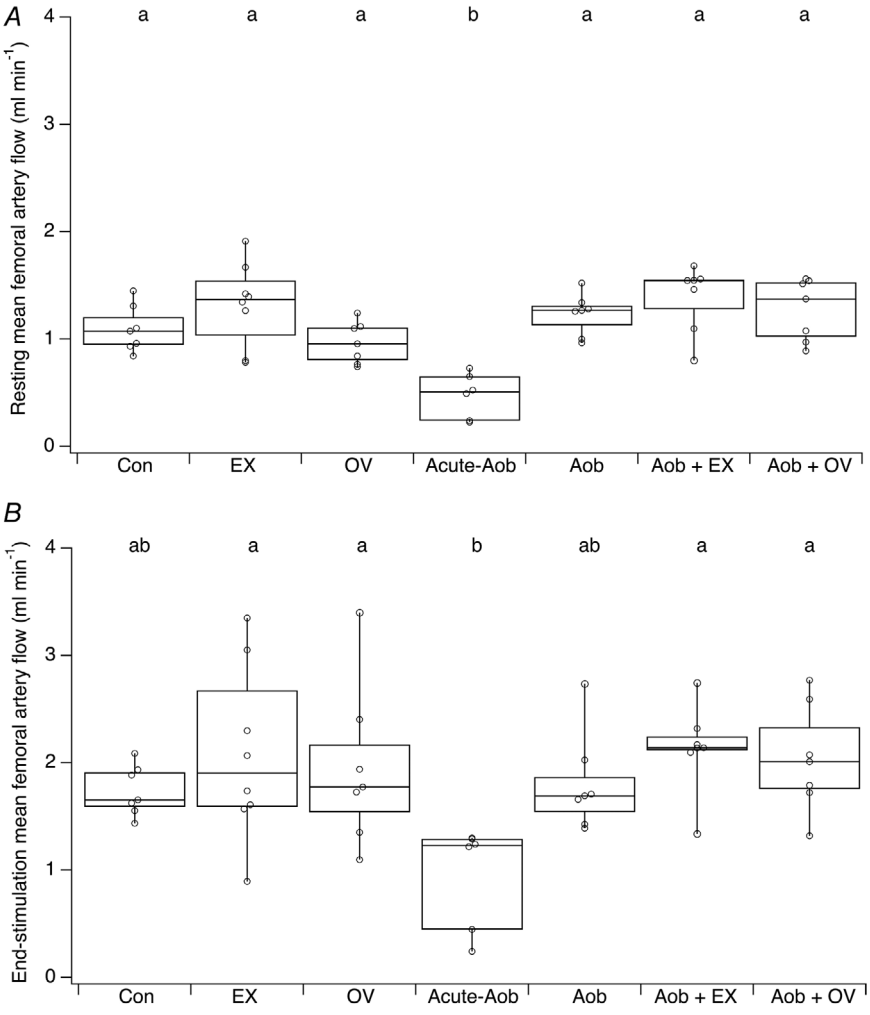

Figure 4. Resting (*A*) and end-stimulation (*B*) mean femoral artery blood flow
A pronounced reduction in femoral blood flow occurred immediately after aortic stenosis (Acute-Aob) but was restored in chronically banded animals. Group sizes were the same as in Fig. 1. Statistically significant differences between groups are denoted by letters; groups sharing the same letter were not different, those sharing none were statistically different ($P < 0.05$) as determined by ANOVA with Tukey's *post hoc* tests.

Table 3. Microcirculatory and muscle fibre morphometric characteristics

	Control	EX	OV	Aob	Aob + EX	Aob + OV
EDL mass (mg per g M_b)	0.56 ± 0.06^{a}	0.61 ± 0.05^{ab}	0.66 ± 0.07^{b}	0.56 ± 0.06^{a}	0.56 ± 0.06^{a}	0.63 ± 0.05^{ab}
Bilateral EDL mass hypertrophy	-	-	1.23 ± 0.11^{a}	-	-	1.12 ± 0.04^{b}
Anatomical capillary density (mm^2)	616 ± 51^{a}	696 ± 123^{ab}	824 ± 142^{b}	606 ± 123^{a}	670 ± 78^{ab}	722 ± 124^{ab}
Perfused capillary density (mm^2)	570 ± 94^{a}	668 ± 116^{a}	728 ± 165^{a}	259 ± 24^{b}	397 ± 95^{b}	366 ± 111^{b}
Anatomical capillary: muscle fibre ratio	1.47 ± 0.30^{ab}	1.41 ± 0.12^{ab}	1.61 ± 0.23^{ab}	1.39 ± 0.39^{a}	1.25 ± 0.11^{a}	1.84 ± 0.22^{b}
Perfused capillary: muscle fibre ratio	1.25 ± 0.29^{ab}	1.36 ± 0.13^{a}	1.42 ± 0.31^{a}	0.63 ± 0.24^{c}	0.76 ± 0.19^{bc}	0.90 ± 0.51^{abc}
Anatomical capillary domain area (μm^2)	1392 ± 119^{a}	1526 ± 268^{ab}	1339 ± 184^{ab}	1888 ± 407^{b}	1547 ± 191^{ab}	1417 ± 201^{a}
Perfused capillary domain area (μm^2)	1823 ± 368^{ab}	1575 ± 287^{a}	1507 ± 225^{a}	4525 ± 586^{c}	2499 ± 641^{ab}	2668 ± 923^{b}
Anatomical $\log_{RSD}$	0.111 ± 0.010^{a}	0.103 ± 0.010^{a}	0.101 ± 0.009^{a}	0.104 ± 0.008^{a}	0.099 ± 0.011^{a}	0.096 ± 0.011^{a}
Perfused $\log_{RSD}$	0.127 ± 0.016^{ab}	0.105 ± 0.010^{a}	0.109 ± 0.010^{ab}	0.131 ± 0.012^{b}	0.124 ± 0.012^{ab}	0.116 ± 0.015^{ab}
EDL fibre composition: Type I (%)	3.9 ± 2.3^{a}	2.2 ± 1.3^{a}	3.5 ± 2.7^{a}	4.4 ± 2.4^{a}	4.8 ± 1.7^{a}	4.1 ± 1.5^{a}
EDL fibre composition: Type IIa (%)	21.9 ± 5.2^{a}	25.3 ± 3.9^{a}	23.2 ± 6.9^{a}	23.5 ± 5.4^{a}	26.3 ± 3.3^{a}	23.3 ± 3.6^{a}
EDL fibre composition: Type IIb/IIx (%)	74.2 ± 7.2^{a}	72.5 ± 4.5^{a}	73.2 ± 9.5^{a}	72.1 ± 7.4^{a}	68.9 ± 3.6^{a}	72.9 ± 3.9^{a}
Type I FCSA (μm^2)	922 ± 217^{a}	922 ± 322^{a}	986 ± 182^{ab}	1151 ± 176^{ab}	969 ± 164^{a}	1340 ± 189^{b}
Type IIa FCSA (μm^2)	939 ± 105^{a}	1102 ± 212^{ab}	1109 ± 133^{ab}	1178 ± 226^{ab}	1054 ± 158^{a}	1379 ± 103^{b}
Type IIb/x FCSA (μm^2)	1754 ± 296^{a}	2520 ± 520^{bc}	2061 ± 187^{abc}	2435 ± 308^{bc}	2079 ± 446^{ab}	2730 ± 447^{c}

Abbreviations: EDL, extensor digitorum longus; $\log_{rSD}$, logarithmic standard deviation of the radius of the capillary domains, i.e. heterogeneity of capillary distribution; FCSA, fibre cross-sectional area. Statistically significant differences between groups across each row are denoted by letters; groups sharing the same letter were not different, those with no shared letters were statistically different ($P < 0.05$) as determined by ANOVA with Tukey's *post hoc* tests.

perfused CDA where a significant increase was found in Aob compared with all other groups ($P < 0.001$). Intervention in Aob+EX ($P = 0.285$) and Aob+OV ($P = 0.103$) reduced this value to levels statistically non-significant from Control (Fig. 5, Table 3).

Neither anatomical Log_{RSD} nor perfused Log_{RSD} were significantly different from Control in any group, and no differences were found amongst Aob, Aob+EX or Aob+OV.

Fibre-type composition did not differ significantly from Control with any intervention. Types I, IIa and IIb/IIx FCSA were, however, larger in Aob+OV when compared with Control (Type I: $P = 0.013$; Type IIa: $P < 0.001$; Type IIb/IIx: $P = 0.001$) and Aob+EX (Type I: $P = 0.035$; Type IIa: $P = 0.013$; Type IIb/IIx: $P = 0.046$), while IIb/IIx fibres were larger than Control in EX ($P = 0.020$), Aob ($P = 0.024$) and Aob+OV ($P = 0.001$) (Table 3). Overload did not change FCSA in OV relative to Control and did not increase in Aob+OV relative to either OV or Aob.

PO_2 modelling

Increased development of potential hypoxic regions within the muscle was observed in Aob, with a pronounced effect at moderate and high-intensity tissue oxygen demand (Fig. 6). Compared with Aob, mean tissue PO_2 was improved in Aob+EX and Aob+OV (Fig. 6*B*), resulting in a qualitative PO_2 distribution similar to that of Control. Within control groups, there was a modest enhancement of tissue PO_2 in EX and OV compared with Con (Fig. 6*A*).

Discussion

In this paper we have demonstrated that CCH coincides with rarefaction of functional capillaries and a reduction in muscle fatigue resistance. Chronic mechanical stretch via overload (analogous to resistance exercise) and voluntary aerobic exercise recovered or prevented loss of perfused capillaries in muscle tissue, thereby contributing

to the maintenance of fatigue resistance. These data indicate that the skeletal muscle microcirculation is a major therapeutic target to restore muscle function in patients with chronic diseases such as CHF.

Effects of acute aortic banding

There was a striking effect of banding and overload or exercise on EDL fatigue resistance, highlighting the sensitivity of skeletal muscle to both local and systemic influences. Aortic banding precipitated an immediate decline in muscle performance that remained reduced in the long term. In the acute situation, reduced muscle fatigue resistance may be due to an attenuated arterial blood supply (corresponding to the low tail blood pressure and reduced exercise-induced FBF), consistent with impaired ischaemic muscle performance in conditions of constrained feed artery perfusion (Fulgenzi *et al.* 1998; Murthy *et al.* 2001).

Effects of chronic aortic banding

The left ventricular pressure overload induced by abdominal aortic coarctation resulted, as expected, in CCH as a consequence of chronic hypertension above the stenosis (Cornelussen *et al.* 1994; Levy *et al.* 1996; De Sousa *et al.* 2002; Degens *et al.* 2006a). Reversal of the observed acute reduction in tail pressure was realized by an increased hypertension indicating that homeostatic mechanisms to maintain peripheral blood pressure were effective during CCH. Yet, muscle fatigue resistance was still reduced 4 weeks after banding despite a normal exercise-induced increase in FBF. We infer that limitations of muscle performance after long-term aortic banding were due to changes within the muscle itself rather than reduced arterial blood supply.

An earlier study using abdominal aortic coarctation-induced CCH reported a muscle-specific effect of CCH on FI, with functional impairments occurring in the soleus and tibialis anterior, but not in the EDL (Levy *et al.* 1996). Although we have no explanation for the discrepancy between EDL performance in this paper and Levy *et al.* (1996), it could be related to methodological differences in the way in which fatigue resistance was determined; 10 Hz stimulation used here elicits a slower decline in force that likely accommodates resolution of fine changes in force, which may be overlooked during the rapid onset of fatigue during 40 Hz stimulation (Levy *et al.* 1996).

We recently demonstrated that perfused capillary density is a major determinant of fatigue resistance in healthy skeletal muscle (Tickle *et al.* 2020), emphasizing that microvascular impairment can contribute to attenuated muscle performance. Capillary rarefaction is associated with impaired exercise tolerance in clinical (Gerovasili *et al.* 2009) heart disease (Duscha *et al.* 1999; Nusz *et al.* 2003) and given the absence of changes in arterial flow in our CCH rodent model, reduction in the perfused muscle microcirculation was a potential constraint on muscle function. Indeed, functional indices of EDL capillarization were negatively affected after development of CCH. Reduced functional (perfused) C:F and CD in Aob also parallels the impaired skeletal muscle blood flow reported in advanced CHF (Wilson *et al.* 1984; Sullivan *et al.* 1989; Musch & Terrell, 1992; Kindig *et al.* 1999). Furthermore, we infer that a larger CDA in Aob compromised fatigue resistance due to diffusion limitations of oxygen (see Fig. 6). The pronounced decline in modelled tissue PO_2 in Aob indicates that rarefaction of perfused vessels imposes a limitation on oxygen diffusion that is exacerbated by exercise of increasing intensity, leading to more rapid muscle fatigue than seen in healthy tissue. That tissue PO_2 is improved after

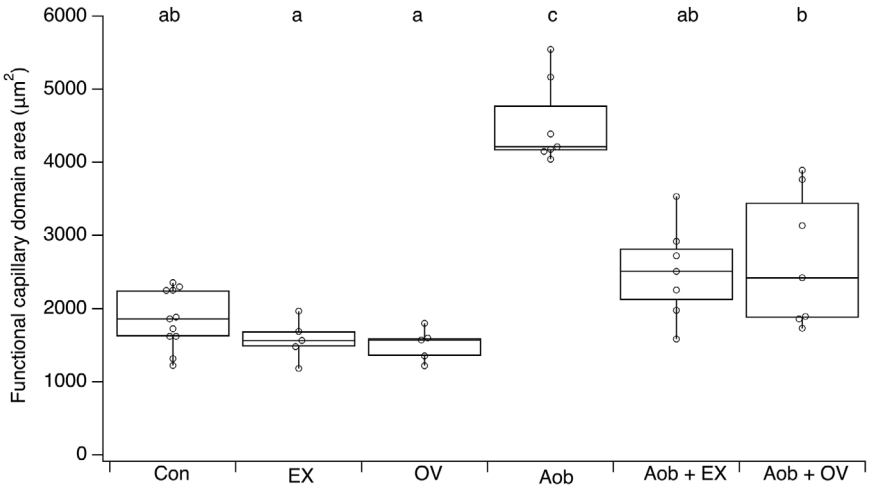

Figure 5. Deleterious enlargement of capillary domain area is restored by angiogenic intervention
Perfused capillary domain area (CDA) is increased after banding (Aob: $N = 7$; $P < 0.01$) but treatment via exercise (Aob+EX: $N = 7$) or overload (Aob+OV: $N = 7$) recovers CDA back to control level ($P > 0.05$). Control ($N = 7$), EX ($N = 5$) and OV ($N = 5$). Statistically significant differences between groups are denoted by letters; groups sharing the same letter were not different, those sharing none were statistically different ($P < 0.05$) as determined by ANOVA with Tukey's *post hoc* tests.

intervention following aortic constriction highlights the potential efficacy of the functional microcirculation for improving fatigue resistance. Interestingly, the PO_2 model outputs broadly correspond to experimental evidence from exercising muscle tissue, whereby a large gradient occurs between capillary and myoglobin-associated PO_2 (Richardson *et al.* 1995; Poole *et al.* 2020).

Despite chronic groups undergoing at least 4 weeks of abdominal aortic constriction, leading to functional microvascular rarefaction, the total (anatomical) C:F

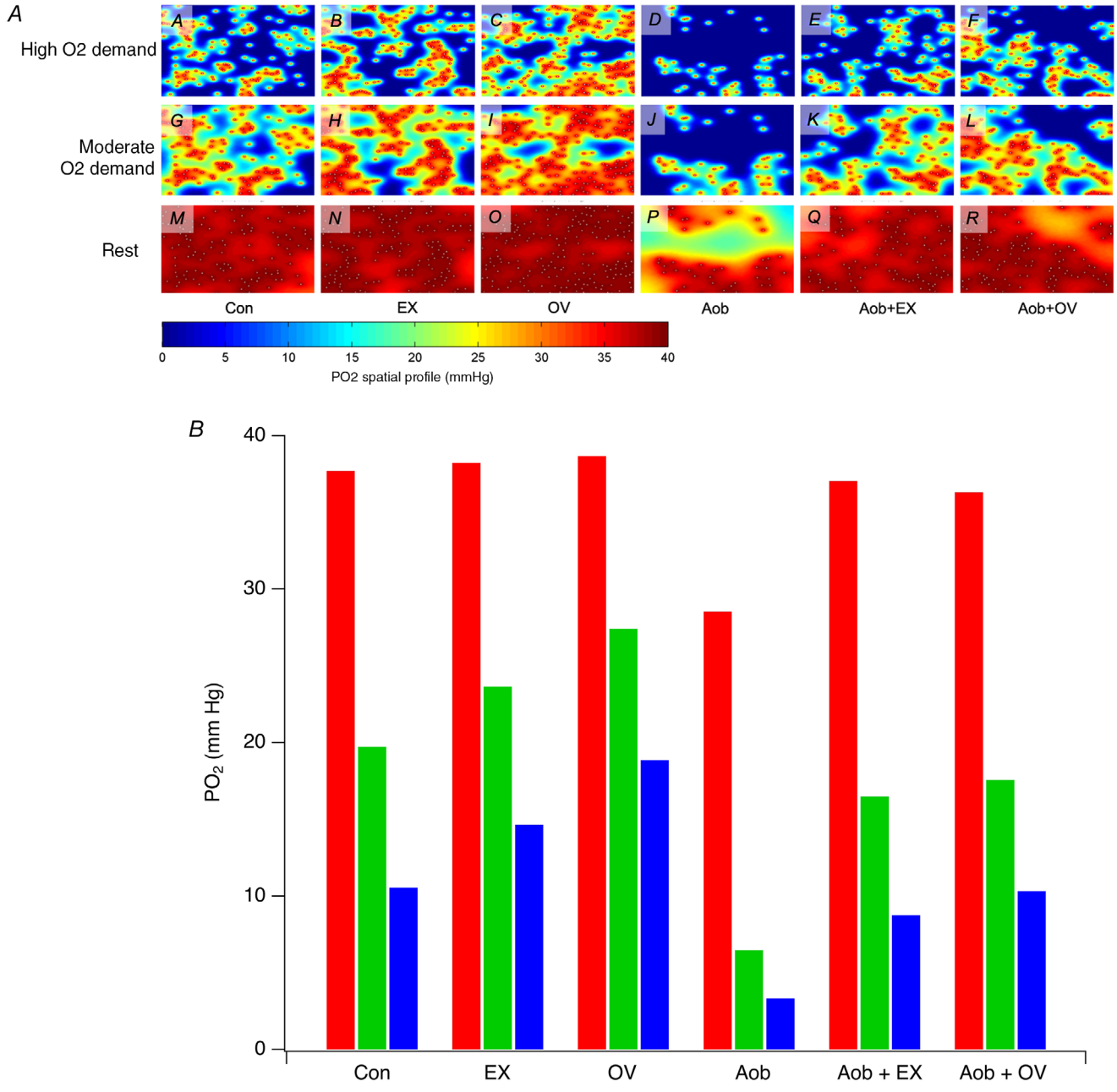

Figure 6. Simulation of muscle PO_2 at rest, moderate and high rates of oxygen consumption
A, based on perfused capillary localization, areas of muscle hypoxia (deep blue shading, where $PO_2 < 0.5$ mmHg) increase after chronic application of an aortic band (Aob: *D*, *J*, *P*) and this pattern corresponds to functional capillary rarefaction and impaired muscle fatigue resistance. Provision of exercise (Aob+EX: *E*, *K*, *Q*) or overload (Aob+OV: *F*, *L*, *R*) improves muscle PO_2 (warmer colours) and provides functional restoration of capillary domain area and muscle fatigue resistance. There is consequently strong evidence for a directional change in PO_2 although simulated absolute PO_2 values should be interpreted with caution due to the inherent limitations of modelling. *B*, average tissue PO_2 during resting (red), moderate (green) and high (blue) intensity tissue O_2 demand. Data were calculated using the exemplar images in (*A*), $N = 1$ in each group. [Colour figure can be viewed at wileyonlinelibrary.com]

and CD were undiminished. This contrasts with other reports of reduced anatomical CD in CHF (Nusz *et al.* 2003), hypertension (Serne *et al.* 2001) and hindlimb ischaemia (Dai *et al.* 2002). While the determinant(s) of this observed reduction in perfused capillaries cannot be specified from the histological data presented in this paper, it appears consistent with an initial (reversible) phase of enhanced vasoconstriction-derived arteriolar closure that, given more time, is followed by structural capillary rarefaction because prolonged hypertension leads to capillary apoptosis (Prewitt *et al.* 1982); therefore our data are likely representative of the incipient phase of microvascular deficit.

Adverse changes in functional capillarity and fatigue resistance in Aob manifested during otherwise normal FBF. Maintenance of femoral flow despite chronic hypertension has been reported in other studies of abdominally coarcted rats with impaired peripheral circulatory structure or function (Overbeck, 1980; Boegehold *et al.* 1991; Levy *et al.* 1996). For example, Boegehold *et al.* (1991) reported peripheral arteriolar rarefaction in the hindlimb of rats subjected to abdominal aortic constriction, despite normal femoral arterial pressure. Similarly, peripheral vascular resistance and impaired hindlimb vasodilation develop after surgically imposed abdominal aortic stenosis, despite no increase in local femoral blood pressure (Bell & Overbeck, 1979; Overbeck, 1980; Ungvari *et al.* 2004). Together, these findings suggest that the mechanism(s) determining functional rarefaction is pressure-independent and therefore derived from systemic factors related to the development of cardiac dysfunction. The established anti-angiogenic effects of reactive oxygen species (Ungvari *et al.* 2004) and inflammatory cytokines (Agnoletti *et al.* 1999; Sun *et al.* 2007), which are both increased during development of cardiac dysfunction, may determine the progression of microvascular rarefaction. This may be further compounded by disuse, as observed in the shorter distanced travelled by Aob+EX, since inactivity leads to microvascular supply deficiency (Kissane *et al.* 2019).

Despite impairments in the functional microcirculation, Log_{RSD} was maintained in Aob, suggesting that, at least in this early phase of CCH and hypertension, heterogeneity of functional and anatomical capillary spacing is unaffected, preventing further declines in oxygen transport and muscle performance (Degens *et al.* 2006b; Al-Shammari *et al.* 2014). Shifts from slow to fast in skeletal muscle fibre type and muscle atrophy may develop with CHF and also contribute to exercise intolerance (Mancini *et al.* 1992; De Sousa *et al.* 2002; Carvalho *et al.* 2003), but these changes did not occur in banded groups. We can therefore exclude these factors as underlying the reduced fatigue resistance in our aortic-banded rats. Changes in fibre type composition are reported to occur 12 weeks after imposition of ascending aortic stenosis and fibre atrophy by 24 weeks (Carvalho *et al.* 2003), so the relatively short 4- to 6-week duration of these experiments may not have been sufficient to observe development of such impairments.

Exercise-mediated preservation of fatigue resistance after aortic banding

Exercise induced an unexpectedly high peripheral blood pressure, contrary to an expected exercise-induced hypotensive effect (Pescatello *et al.* 1991). Compared with Control, there was also an adaptive cardiac enlargement with exercise (EX) that did not significantly differ in magnitude from the reactive hypertrophy in Aob+EX and Aob+OV, indicating the potential contributions of adaptive (Moreira-Goncalves *et al.* 2015) and pathological (Grossman *et al.* 1975) stimuli to cardiac growth.

Wheel-running exercise did not significantly enhance FI in EX animals, but maintained muscle performance in Aob+EX despite development of CCH. This suggests that the level of exercise completed by animals was not sufficient to register an improvement in the exercise tolerance of the EDL muscle in EX, but was of sufficient intensity to offset the pathological effects of CCH on skeletal muscle in Aob. While inclination to exercise was undiminished in Aob+EX, the duration and intensity of each running bout was lower than in EX, leading to a lower overall distance travelled, mirroring previous work in banded rats (De Sousa *et al.* 2002). Interestingly, mean running velocity was reduced relative to EX in Aob+EX indicating that onset of volitional exercise fatigue contributed to declining (expected) locomotor muscle power output, despite no differences in maximal isometric twitch tension, i.e. muscle force generation was not impaired *per se*, but other factors compromised functional output. Nevertheless, the lesser amount of exercise was sufficient to restore EDL function to normal levels, thereby highlighting the beneficial effect of limited aerobic activity to reverse pathological changes that occur in skeletal muscle with CCH. Abnormalities in mitochondrial function and muscle metabolism are also reversed following voluntary exercise in clinical CHF (Adamopoulos *et al.* 1993; Stratton *et al.* 1994; Hambrecht *et al.* 1995) and an aortic coarctation model (De Sousa *et al.* 2002; Gomes *et al.* 2016), so together these data indicate that aerobic exercise provides a potent restorative effect on skeletal muscle structure and function in various stages of disease.

Voluntary wheel-running did not confer obvious benefit on structural or functional muscle microvasculature in unbanded rats, and in line with this, muscle FI in EX was not significantly different from Control. It is recognized that the pro-angiogenic effects of exercise may not be activated below a critical threshold

(Prior *et al.* 2003), so it is perhaps not surprising that low-intensity wheel-running did not stimulate significant capillary proliferation in EX. In contrast, aerobic exercise after banding (Aob+EX) preserved functional CDA and perfused C:F, thereby maintaining tissue oxygenation and normal muscle FI (Al-Shammari *et al.* 2014). Therefore, low-intensity aerobic exercise may stimulate the reopening of hypertension-derived vasoconstricted arterioles to allow for utilization of the underlying functional microcirculation. The vasodilatory effects of an increased production of nitric oxide (Koller *et al.* 1994) and prostaglandins (Murrant *et al.* 2014) during exercise may determine this potential for increased capillary availability. Interestingly, although $\log_{RSD}$ was maintained, perfused CD remained below unbanded levels in Aob+EX indicating that microvascular remodelling after exercise may be targeted to restore capillarity to meet local functional requirements. Establishment of local hypoxic regions within muscle upon microvascular rarefaction with CCH (Fig. 6) may also contribute to a potentiated angiogenic response because hypoxic and exercise stimuli occur simultaneously, activating multiple proliferation pathways (Adair, 2005). Many of the reported benefits of exercise therapy in CHF (Belardinelli *et al.* 1999) may therefore be in part due to microvascular remodelling.

Recovery of fatigue resistance by overload after aortic banding

OV enhanced FI, as found in previous experimental studies (Frischknecht & Vrbova, 1991; Degens *et al.* 1993; Tickle *et al.* 2020). This benefit extended to animals with CCH, where an FI improvement of *ca* 32% was recorded in Aob+OV compared with a 25% enhancement in OV. In this case, therefore, a targeted mechanical stimulus without (obvious) systemic reciprocal effects leads to a rapid restoration of muscle performance. This parallels the enhanced muscle performance in CHF patients after resistance exercise therapy (Selig *et al.* 2004; Braith *et al.* 2005; Braith & Beck, 2008; Giuliano *et al.* 2017).

Improved functional capillarity with overload was accompanied by enhanced fatigue resistance, as reported previously (Degens *et al.* 1992; Zhou *et al.* 1998; Deveci & Egginton, 2002; Egginton *et al.* 2011; Ballak *et al.* 2016; Tickle *et al.* 2020), and parallels the upregulation of angiogenic growth factor expression and capillarity observed after resistance exercise in healthy subjects (Gavin *et al.* 2007; Ferguson *et al.* 2018; Holloway *et al.* 2018) and CHF patients (Williams *et al.* 2007). Alleviation of symptoms associated with heart disease may be hampered by coincident pathologies such as impaired peripheral blood flow, reducing the angiogenic effects of hyperaemic stimuli for expansion of the microcirculation. Interestingly, angiogenesis following overload may occur in conditions of experimentally reduced blood flow (Egginton *et al.* 1998; Deveci & Egginton, 2002), highlighting the potential of flow-independent mechanical stimuli to improve muscle capillarity and fatigue resistance, even in advanced disease. Therefore, angiogenesis may contribute to improved capillary perfusion by increasing the anatomical supply of microvessels fed by patent arterioles, or elevated angiogenic growth factor levels may attenuate capillary apoptosis. This may occur in the sedentary overload model despite a relative lack of shear stress-derived nitric oxide and prostaglandin upregulation, which may otherwise contribute to a reopening of constricted arterioles with aerobic exercise intervention. The successful application of muscle overload to rats with CCH provides further evidence to support therapeutic resistance exercise, which has the benefit of imparting additional cardiovascular strain for short bouts in contrast to the long durations required with aerobic exercise (Duncker *et al.* 2014) while providing an effective method for improving muscle function (Giuliano *et al.* 2017).

While EDL hypertrophy occurred in OV and Aob+OV, relative mass gain was lower after development of CCH although there were no significant differences in maximal twitch force or FCSA. Impaired muscle hypertrophy with induced CCH is similar to that reported in a rat model of metabolic syndrome, where limited overload-induced muscle growth was attributed to dysfunctional mTOR signalling, a central regulator of growth and proliferation (Katta *et al.* 2010; Paturi *et al.* 2010). Raised levels of inflammatory cytokines, particularly TNFα, suppress mTOR activity in heart failure (Seiler *et al.* 2016) and may in part explain reduced gain in muscle mass in Aob+OV (Schiaffino *et al.* 2013).

Greater capillarization is associated with enhanced skeletal muscle fibre hypertrophy after resistance exercise training (Snijders *et al.* 2017; Moro *et al.* 2019), highlighting the critical importance of the microcirculation to muscle growth. Reduced functional capillarization with CCH may therefore contribute to the blunted hypertrophic response. Given the potential for regrowth of the functional microcirculation in Aob+OV, a longer period of overload may accommodate a full restoration of capillary parameters.

Conclusion

We have demonstrated that functional microvascular rarefaction with CCH underlies the impaired skeletal muscle fatigue resistance in CCH. Loss of functional capillarization can, however, be prevented through aerobic exercise and restored by functional overload-derived angiogenic stimuli, contributing to the successful recovery of muscle performance. Therefore, improved fatigue

resistance in Aob+EX and Aob+OV as a consequence of improved functional capillarity supports the hypothesis that skeletal muscle performance in CHF is primarily determined by peripheral factors, specifically the muscle microcirculation. These interpretations bear a caveat: we have determined the effects on skeletal muscle function of incipient cardiac dysfunction rather than advanced disease, when co-morbidities add complexity to the mechanisms of muscle dysfunction. Nevertheless, the key determining role of muscle microcirculation in the development of exercise impairments during cardiac dysfunction underscore how angiogenic restorative growth should be a key therapeutic target.

References

Adair TH (2005). Growth regulation of the vascular system: an emerging role for adenosine. *Am J Physiol Regul Integr Comp Physiol* **289**, R283–R296.

Adamopoulos S, Coats AJ, Brunotte F, Arnolda L, Meyer T, Thompson CH, Dunn JF, Stratton J, Kemp GJ, Radda GK & Rajagopalan B (1993). Physical training improves skeletal muscle metabolism in patients with chronic heart failure. *J Am Coll Cardiol* **21**, 1101–1106.

Agnoletti L, Curello S, Bachetti T, Malacarne F, Gaia G, Comini L, Volterrani M, Bonetti P, Parrinello G, Cadei M, Grigolato PG & Ferrari R (1999). Serum from patients with severe heart failure downregulates eNOS and is proapoptotic: role of tumor necrosis factor-alpha. *Circulation* **100**, 1983–1991.

Al-Shammari AA, Gaffney EA & Egginton S (2014). Modelling capillary oxygen supply capacity in mixed muscles: capillary domains revisited. *J Theor Biol* **356**, 47–61.

Al-Shammari AA, Kissane RWP, Holbek S, Mackey AL, Andersen TR, Gaffney EA, Kjaer M & Egginton S (2019). Integrated method for quantitative morphometry and oxygen transport modeling in striated muscle. *J Appl Physiol* **126**, 544–557.

Andersen P & Henriksson J (1977). Capillary supply of the quadriceps femoris muscle of man: adaptive response to exercise. *J Physiol* **270**, 677–690.

Arakawa H, Ikeda U, Hojo Y, Ueno S, Nonaka-Sarukawa M, Yamamoto K & Shimada K (2003). Decreased serum vascular endothelial growth factor concentrations in patients with congestive heart failure. *Heart* **89**, 207–208.

Ballak SB, Buse-Pot T, Harding PJ, Yap MH, Deldicque L, de Haan A, Jaspers RT & Degens H (2016). Blunted angiogenesis and hypertrophy are associated with increased fatigue resistance and unchanged aerobic capacity in old overloaded mouse muscle. *Age* **38**, 39.

Behnke BJ, Delp MD, Poole DC & Musch TI (2007). Aging potentiates the effect of congestive heart failure on muscle microvascular oxygenation. *J Appl Physiol* **103**, 1757–1763.

Belardinelli R, Georgiou D, Cianci G & Purcaro A (1999). Randomized, controlled trial of long-term moderate exercise training in chronic heart failure: effects on functional capacity, quality of life, and clinical outcome. *Circulation* **99**, 1173–1182.

Bell DR & Overbeck HW (1979). Increased resistance and impaired maximal vasodilation in normotensive vascular beds of rats with coarctation hypertension. *Hypertension* **1**, 78–85.

Boegehold MA, Johnson MD & Overbeck HW (1991). Pressure-independent arteriolar rarefaction in hypertension. *Am J Physiol* **261**, H83–87.

Bowen TS, Brauer D, Rolim NPL, Baekkerud FH, Kricke A, Ormbostad Berre AM, Fischer T, Linke A, da Silva GJ, Wisloff U & Adams V (2017). Exercise training reveals inflexibility of the diaphragm in an animal model of patients with obesity-driven heart failure with a preserved ejection fraction. *J Am Heart Assoc* **6**, e006416.

Braith RW & Beck DT (2008). Resistance exercise: training adaptations and developing a safe exercise prescription. *Heart Fail Rev* **13**, 69–79.

Braith RW, Magyari PM, Pierce GL, Edwards DG, Hill JA, White LJ & Aranda JM, Jr (2005). Effect of resistance exercise on skeletal muscle myopathy in heart transplant recipients. *Am J Cardiol* **95**, 1192–1198.

Brodal P, Ingjer F & Hermansen L (1977). Capillary supply of skeletal muscle fibers in untrained and endurance-trained men. *Am J Physiol* **232**, H705–712.

Carvalho RF, Cicogna AC, Campos GE, De Assis JM, Padovani CR, Okoshi MP & Pai-Silva MD (2003). Myosin heavy chain expression and atrophy in rat skeletal muscle during transition from cardiac hypertrophy to heart failure. *Int J Exp Pathol* **84**, 201–206.

Chong AY, Caine GJ & Lip GY (2004). Angiopoietin/tie-2 as mediators of angiogenesis: a role in congestive heart failure?. *Eur J Clin Invest* **34**, 9–13.

Cornelussen R, Spiering W, Webers JH, De Bruin LG, Reneman RS, van der Vusse GJ & Snoeckx LH (1994). Heat shock improves ischemic tolerance of hypertrophied rat hearts. *Am J Physiol* **267**, H1941–1947.

Dai Q, Thompson MA, Pippen AM, Cherwek H, Taylor DA & Annex BH (2002). Alterations in endothelial cell proliferation and apoptosis contribute to vascular remodeling following hind-limb ischemia in rabbits. *Vasc Med* **7**, 87–91.

De Sousa E, Lechene P, Fortin D, N'Guessan B, Belmadani S, Bigard X, Veksler V & Ventura-Clapier R (2002). Cardiac and skeletal muscle energy metabolism in heart failure: beneficial effects of voluntary activity. *Cardiovasc Res* **56**, 260–268.

Degens H, de Brouwer KF, Gilde AJ, Lindhout M, Willemsen PH, Janssen BJ, van der Vusse GJ & van Bilsen M (2006*a*). Cardiac fatty acid metabolism is preserved in the compensated hypertrophic rat heart. *Basic Res Cardiol* **101**, 17–26.

Degens H, Deveci D, Botto-van Bemden A, Hoofd LJ & Egginton S (2006*b*). Maintenance of heterogeneity of capillary spacing is essential for adequate oxygenation in the soleus muscle of the growing rat. *Microcirculation* **13**, 467–476.

Degens H, Turek Z, Hoofd LJ, Van't Hof MA & Binkhorst RA (1992). The relationship between capillarisation and fibre types during compensatory hypertrophy of the plantaris muscle in the rat. *J Anat* **180** 455–463.

Degens H, Veerkamp JH, van Moerkerk HT, Turek Z, Hoofd LJ & Binkhorst RA (1993). Metabolic capacity, fibre type area and capillarization of rat plantaris muscle. Effects of age, overload and training and relationship with fatigue resistance. *Int J Biochem* **25**, 1141–1148.

Deveci D & Egginton S (2002). Muscle ischaemia in rats may be relieved by overload-induced angiogenesis. *Exp Physiol* **87**, 479–488.

Drexler H, Riede U, Munzel T, Konig H, Funke E & Just H (1992). Alterations of skeletal muscle in chronic heart failure. *Circulation* **85**, 1751–1759.

Duncker DJ, van Deel ED, de Waard MC, de Boer M, Merkus D & van der Velden J (2014). Exercise training in adverse cardiac remodeling. *Pflugers Arch* **466**, 1079–1091.

Duscha BD, Kraus WE, Keteyian SJ, Sullivan MJ, Green HJ, Schachat FH, Pippen AM, Brawner CA, Blank JM & Annex BH (1999). Capillary density of skeletal muscle: a contributing mechanism for exercise intolerance in class II-III chronic heart failure independent of other peripheral alterations. *J Am Coll Cardiol* **33**, 1956–1963.

Egginton S, Badr I, Williams J, Hauton D, Baan GC & Jaspers RT (2011). Physiological angiogenesis is a graded, not threshold, response. *J Physiol* **589**, 195–206.

Egginton S & Hudlicka O (1999). Early changes in performance, blood flow and capillary fine structure in rat fast muscles induced by electrical stimulation. *J Physiol* **515**, 265–275.

Egginton S, Hudlicka O, Brown MD, Walter H, Weiss JB & Bate A (1998). Capillary growth in relation to blood flow and performance in overloaded rat skeletal muscle. *J Appl Physiol* **85**, 2025–2032.

Egginton S, Hussain A, Hall-Jones J, Chaudhry B, Syeda F & Glen KE (2016). Shear stress-induced angiogenesis in mouse muscle is independent of the vasodilator mechanism and quickly reversible. *Acta Physiol* **218**, 153–166.

Egginton S, Zhou AL, Brown MD & Hudlicka O (2001). Unorthodox angiogenesis in skeletal muscle. *Cardiovasc Res* **49**, 634–646.

Esposito F, Mathieu-Costello O, Entin PL, Wagner PD & Richardson RS (2010). The skeletal muscle VEGF mRNA response to acute exercise in patients with chronic heart failure. *Growth Factors* **28**, 139–147.

Esposito F, Mathieu-Costello O, Wagner PD & Richardson RS (2018). Acute and chronic exercise in patients with heart failure with reduced ejection fraction: evidence of structural and functional plasticity and intact angiogenic signalling in skeletal muscle. *J Physiol* **596**, 5149–5161.

Ferguson RA, Hunt JEA, Lewis MP, Martin NRW, Player DJ, Stangier C, Taylor CW & Turner MC (2018). The acute angiogenic signalling response to low-load resistance exercise with blood flow restriction. *Eur J Sport Sci* **18**, 397–406.

Franciosa JA, Park M & Levine TB (1981). Lack of correlation between exercise capacity and indexes of resting left ventricular performance in heart failure. *Am J Cardiol* **47**, 33–39.

Frischknecht R & Vrbova G (1991). Adaptation of rat extensor digitorum longus to overload and increased activity. *Pflugers Arch* **419**, 319–326.

Fulgenzi G, Graciotti L, Collis MG & Hudlicka O (1998). The effect of alpha 1 adrenoceptor antagonist prazosin on capillary supply, blood flow and performance in a rat model of chronic muscle ischaemia. *Eur J Vasc Endovasc Surg* **16**, 71–77.

Gavin TP, Drew JL, Kubik CJ, Pofahl WE & Hickner RC (2007). Acute resistance exercise increases skeletal muscle angiogenic growth factor expression. *Acta Physiol* **191**, 139–146.

Gerovasili V, Drakos S, Kravari M, Malliaras K, Karatzanos E, Dimopoulos S, Tasoulis A, Anastasiou-Nana M, Roussos C & Nanas S (2009). Physical exercise improves the peripheral microcirculation of patients with chronic heart failure. *J Cardiopulm Rehabil Prev* **29**, 385–391.

Giuliano C, Karahalios A, Neil C, Allen J & Levinger I (2017). The effects of resistance training on muscle strength, quality of life and aerobic capacity in patients with chronic heart failure - A meta-analysis. *Int J Cardiol* **227**, 413–423.

Goldspink DF, Cox VM, Smith SK, Eaves LA, Osbaldeston NJ, Lee DM & Mantle D (1995). Muscle growth in response to mechanical stimuli. *Am J Physiol* **268**, E288–297.

Gomes MJ, Martinez PF, Campos DH, Pagan LU, Bonomo C, Lima AR, Damatto RL, Cezar MD, Damatto FC, Rosa CM, Garcia CM, Reyes DR, Fernandes AA, Fernandes DC, Laurindo FR, Okoshi K & Okoshi MP (2016). Beneficial effects of physical exercise on functional capacity and skeletal muscle oxidative stress in rats with aortic stenosis-induced heart failure. *Oxid Med Cell Longev* **2016**, 8695716.

Grossman W, Jones D & McLaurin LP (1975). Wall stress and patterns of hypertrophy in the human left ventricle. *J Clin Invest* **56**, 56–64.

Grundy D (2015). Principles and standards for reporting animal experiments in The Journal of Physiology and Experimental Physiology. *J Physiol* **593**, 2547–2549.

Gustafsson T, Bodin K, Sylven C, Gordon A, Tyni-Lenne R & Jansson E (2001). Increased expression of VEGF following exercise training in patients with heart failure. *Eur J Clin Invest* **31**, 362–366.

Hambrecht R, Niebauer J, Fiehn E, Kalberer B, Offner B, Hauer K, Riede U, Schlierf G, Kubler W & Schuler G (1995). Physical training in patients with stable chronic heart failure: effects on cardiorespiratory fitness and ultrastructural abnormalities of leg muscles. *J Am Coll Cardiol* **25**, 1239–1249.

Hauton D, Winter J, Al-Shammari AA, Gaffney EA, Evans RD & Egginton S (2015). Changes to both cardiac metabolism and performance accompany acute reductions in functional capillary supply. *Biochim Biophys Acta* **1850**, 681–690.

Haykowsky MJ, Brubaker PH, Stewart KP, Morgan TM, Eggebeen J & Kitzman DW (2012). Effect of endurance training on the determinants of peak exercise oxygen consumption in elderly patients with stable compensated heart failure and preserved ejection fraction. *J Am Coll Cardiol* **60**, 120–128.

Holloway TM, Snijders T, van Kranenburg J, van Loon LJC, & Verdijk LB (2018). Temporal response of angiogenesis and hypertrophy to resistance training in young men. *Med Sci Sports Exerc* **50**, 36–45.

Hoofd L, Turek Z, Kubat K, Ringnalda BE & Kazda S (1985). Variability of intercapillary distance estimated on histological sections of rat heart. *Adv Exp Med Biol* **191**, 239–247.

Hudlicka O (1991). What makes blood vessels grow?. *J Physiol* **444**, 1–24.

Hudlicka O, Brown M, Cotter M, Smith M & Vrbova G (1977). The effect of long-term stimulation of fast muscles on their blood flow, metabolism and ability to withstand fatigue. *Pflugers Arch* **369**, 141–149.

Katta A, Kundla S, Kakarla SK, Wu M, Fannin J, Paturi S, Liu H, Addagarla HS & Blough ER (2010). Impaired overload-induced hypertrophy is associated with diminished mTOR signaling in insulin-resistant skeletal muscle of the obese Zucker rat. *Am J Physiol Regul Integr Comp Physiol* **299**, R1666–R1675.

Katz SD, Maskin C, Jondeau G, Cocke T, Berkowitz R & LeJemtel T (2000). Near-maximal fractional oxygen extraction by active skeletal muscle in patients with chronic heart failure. *J Appl Physiol* **88**, 2138–2142.

Kindig CA, Musch TI, Basaraba RJ & Poole DC (1999). Impaired capillary hemodynamics in skeletal muscle of rats in chronic heart failure. *J Appl Physiol* **87**, 652–660.

Kissane RWP, Egginton S & Askew GN (2018). Regional variation in the mechanical properties and fibre-type composition of the rat extensor digitorum longus muscle. *Exp Physiol* **103**, 111–124.

Kissane RWP, Tickle PG, Doody NE, Al-Shammari AA & Egginton S (2021). Distinct structural and functional angiogenic responses are induced by different mechanical stimuli. *Microcirculation*, e12677.

Kissane RWP, Wright O, Al'Joboori YD, Marczak P, Ichiyama RM & Egginton S (2019). Effects of treadmill training on microvascular remodeling in the rat after spinal cord injury. *Muscle Nerve* **59**, 370–379.

Koller A, Sun D, Huang A & Kaley G (1994). Corelease of nitric oxide and prostaglandins mediates flow-dependent dilation of rat gracilis muscle arterioles. *Am J Physiol* **267**, H326–332.

Levy LB, Avkiran M, Ferrari R & Hearse DJ (1996). Impaired skeletal muscle fatigue resistance in rats with pressure overload-induced left ventricular hypertrophy. *J Mol Cell Cardiol* **28**, 183–195.

Mancini DM, Walter G, Reichek N, Lenkinski R, McCully KK, Mullen JL & Wilson JR (1992). Contribution of skeletal muscle atrophy to exercise intolerance and altered muscle metabolism in heart failure. *Circulation* **85**, 1364–1373.

Mandel ER, Dunford EC, Trifonova A, Abdifarkosh G, Teich T, Riddell MC & Haas TL (2016). Prazosin can prevent glucocorticoid mediated capillary rarefaction. *PLoS One* **11**, e0166899.

Moreira-Goncalves D, Henriques-Coelho T, Fonseca H, Ferreira R, Padrao AI, Santa C, Vieira S, Silva AF, Amado F, Leite-Moreira A & Duarte JA (2015). Intermittent cardiac overload results in adaptive hypertrophy and provides protection against left ventricular acute pressure overload insult. *J Physiol* **593**, 3885–3897.

Moro T, Brightwell CR, Phalen DE, McKenna CF, Lane SJ, Porter C, Volpi E, Rasmussen BB & Fry CS (2019). Low skeletal muscle capillarization limits muscle adaptation to resistance exercise training in older adults. *Exp Gerontol* **127**, 110723.

Murrant CL, Dodd JD, Foster AJ, Inch KA, Muckle FR, Ruiz DA, Simpson JA & Scholl JH (2014). Prostaglandins induce vasodilatation of the microvasculature during muscle contraction and induce vasodilatation independent of adenosine. *J Physiol* **592**, 1267–1281.

Murthy G, Hargens AR, Lehman S & Rempel DM (2001). Ischemia causes muscle fatigue. *J Orthop Res* **19**, 436–440.

Musch TI & Terrell JA (1992). Skeletal muscle blood flow abnormalities in rats with a chronic myocardial infarction: rest and exercise. *Am J Physiol* **262**, H411–419.

Nusz DJ, White DC, Dai Q, Pippen AM, Thompson MA, Walton GB, Parsa CJ, Koch WJ & Annex BH (2003). Vascular rarefaction in peripheral skeletal muscle after experimental heart failure. *Am J Physiol Heart Circ Physiol* **285**, H1554–H1562.

Olesen J, Kiilerich K & Pilegaard H (2010). PGC-1alpha-mediated adaptations in skeletal muscle. *Pflugers Arch* **460**, 153–162.

Olfert IM, Baum O, Hellsten Y & Egginton S (2016). Advances and challenges in skeletal muscle angiogenesis. *Am J Physiol Heart Circ Physiol* **310**, H326–H336.

Overbeck HW (1980). Pressure-independent increases in vascular resistance in hypertension: role of sympathoadrenergic influences. *Hypertension* **2**, 780–786.

Pandey A, Parashar A, Kumbhani D, Agarwal S, Garg J, Kitzman D, Levine B, Drazner M & Berry J (2015). Exercise training in patients with heart failure and preserved ejection fraction: meta-analysis of randomized control trials. *Circ Heart Fail* **8**, 33–40.

Paturi S, Gutta AK, Kakarla SK, Katta A, Arnold EC, Wu M, Rice KM & Blough ER (2010). Impaired overload-induced hypertrophy in obese Zucker rat slow-twitch skeletal muscle. *J Appl Physiol* **108**, 7–13.

Pescatello LS, Fargo AE, Leach CN, Jr. & Scherzer HH (1991). Short-term effect of dynamic exercise on arterial blood pressure. *Circulation* **83**, 1557–1561.

Piiper J & Scheid P (1991). Diffusion limitation of O2 supply to tissue in homogeneous and heterogeneous models. *Respir Physiol* **85**, 127–136.

Poole DC, Pittman RN, Musch TI & Ostergaard L (2020). August Krogh's theory of muscle microvascular control and oxygen delivery: a paradigm shift based on new data. *J Physiol* **598**, 4473–4507.

Prewitt RL, Chen, II & Dowell R (1982). Development of microvascular rarefaction in the spontaneously hypertensive rat. *Am J Physiol* **243**, H243–251.

Prior BM, Lloyd PG, Yang HT & Terjung RL (2003). Exercise-induced vascular remodeling. *Exerc Sport Sci Rev* **31**, 26–33.

Ranjbar K, Ardakanizade M & Nazem F (2017). Endurance training induces fiber type-specific revascularization in hindlimb skeletal muscles of rats with chronic heart failure. *Iran J Basic Med Sci* **20**, 90–98.

Richardson RS, Noyszewski EA, Kendrick KF, Leigh JS & Wagner PD (1995). Myoglobin O2 desaturation during exercise. Evidence of limited O2 transport. *J Clin Invest* **96**, 1916–1926.

Richardson TE, Kindig CA, Musch TI & Poole DC (2003). Effects of chronic heart failure on skeletal muscle capillary hemodynamics at rest and during contractions. *J Appl Physiol* **95**, 1055–1062.

Rogers FJ (2001). The muscle hypothesis: a model of chronic heart failure appropriate for osteopathic medicine. *J Am Osteopath Assoc* **101**, 576–583.

Rossig L, Haendeler J, Mallat Z, Hugel B, Freyssinet JM, Tedgui A, Dimmeler S & Zeiher AM (2000). Congestive heart failure induces endothelial cell apoptosis: protective role of carvedilol. *J Am Coll Cardiol* **36**, 2081–2089.

Schaufelberger M, Eriksson BO, Grimby G, Held P & Swedberg K (1995). Skeletal muscle fiber composition and capillarization in patients with chronic heart failure: relation to exercise capacity and central hemodynamics. *J Card Fail* **1**, 267–272.

Schiaffino S, Dyar KA, Ciciliot S, Blaauw B & Sandri M (2013). Mechanisms regulating skeletal muscle growth and atrophy. *FEBS J* **280**, 4294–4314.

Seiler M, Bowen TS, Rolim N, Dieterlen MT, Werner S, Hoshi T, Fischer T, Mangner N, Linke A, Schuler G, Halle M, Wisloff U & Adams V (2016). Skeletal muscle alterations are exacerbated in heart failure with reduced compared with preserved ejection fraction: mediated by circulating cytokines?. *Circ Heart Fail* **9**, e003027.

Selig SE, Carey MF, Menzies DG, Patterson J, Geerling RH, Williams AD, Bamroongsuk V, Toia D, Krum H & Hare DL (2004). Moderate-intensity resistance exercise training in patients with chronic heart failure improves strength, endurance, heart rate variability, and forearm blood flow. *J Card Fail* **10**, 21–30.

Serne EH, Gans RO, ter Maaten JC, Tangelder GJ, Donker AJ & Stehouwer CD (2001). Impaired skin capillary recruitment in essential hypertension is caused by both functional and structural capillary rarefaction. *Hypertension* **38**, 238–242.

Snijders T, Nederveen JP, Joanisse S, Leenders M, Verdijk LB, van Loon LJ & Parise G (2017). Muscle fibre capillarization is a critical factor in muscle fibre hypertrophy during resistance exercise training in older men. *J Cachexia Sarcopenia Muscle* **8**, 267–276.

Snyder GK, Wilcox EE & Burnham EW (1985). Effects of hypoxia on muscle capillarity in rats. *Respir Physiol* **62**, 135–140.

Solomon S & Bengele HH (1973). Growth rates and organ weights of rats. *Biol Neonate* **22**, 222–229.

Stratton JR, Dunn JF, Adamopoulos S, Kemp GJ, Coats AJ & Rajagopalan B (1994). Training partially reverses skeletal muscle metabolic abnormalities during exercise in heart failure. *J Appl Physiol* **76**, 1575–1582.

Sullivan MJ, Knight JD, Higginbotham MB & Cobb FR (1989). Relation between central and peripheral hemodynamics during exercise in patients with chronic heart failure. Muscle blood flow is reduced with maintenance of arterial perfusion pressure. *Circulation* **80**, 769–781.

Sun M, Chen M, Dawood F, Zurawska U, Li JY, Parker T, Kassiri Z, Kirshenbaum LA, Arnold M, Khokha R & Liu PP (2007). Tumor necrosis factor-alpha mediates cardiac remodeling and ventricular dysfunction after pressure overload state. *Circulation* **115**, 1398–1407.

Tickle PG, Hendrickse PW, Degens H & Egginton S (2020). Impaired skeletal muscle performance as a consequence of random functional capillary rarefaction can be restored with overload-dependent angiogenesis. *J Physiol* **598**, 1187–1203.

Ungvari Z, Csiszar A, Kaminski PM, Wolin MS & Koller A (2004). Chronic high pressure-induced arterial oxidative stress: involvement of protein kinase C-dependent NAD(P)H oxidase and local renin-angiotensin system. *Am J Pathol* **165**, 219–226.

Valgimigli M, Rigolin GM, Fucili A, Porta MD, Soukhomovskaia O, Malagutti P, Bugli AM, Bragotti LZ, Francolini G, Mauro E, Castoldi G & Ferrari R (2004). CD34+ and endothelial progenitor cells in patients with various degrees of congestive heart failure. *Circulation* **110**, 1209–1212.

Wadowski PP, Hulsmann M, Schorgenhofer C, Lang IM, Wurm R, Gremmel T, Koppensteiner R, Steinlechner B, Schwameis M & Jilma B (2018). Sublingual functional capillary rarefaction in chronic heart failure. *Eur J Clin Invest* **48**, e12869.

Waters RE, Rotevatn S, Li P, Annex BH & Yan Z (2004). Voluntary running induces fiber type-specific angiogenesis in mouse skeletal muscle. *Am J Physiol Cell Physiol* **287**, C1342-C1348.

Williams AD, Carey MF, Selig S, Hayes A, Krum H, Patterson J, Toia D & Hare DL (2007). Circuit resistance training in chronic heart failure improves skeletal muscle mitochondrial ATP production rate–a randomized controlled trial. *J Card Fail* **13**, 79–85.

Williams JL, Weichert A, Zakrzewicz A, Da Silva-Azevedo L, Pries AR, Baum O & Egginton S (2006). Differential gene and protein expression in abluminal sprouting and intraluminal splitting forms of angiogenesis. *Clin Sci* **110**, 587–595.

Wilson JR, Martin JL, Schwartz D & Ferraro N (1984). Exercise intolerance in patients with chronic heart failure: role of impaired nutritive flow to skeletal muscle. *Circulation* **69**, 1079–1087.

Zhou AL, Egginton S, Brown MD & Hudlicka O (1998). Capillary growth in overloaded, hypertrophic adult rat skeletal muscle: an ultrastructural study. *Anat Rec* **252**, 49–63.

Zumstein A, Mathieu O, Howald H & Hoppeler H (1983). Morphometric analysis of the capillary supply in skeletal muscles of trained and untrained subjects–its limitations in muscle biopsies. *Pflugers Arch* **397**, 277–283.

Additional information

Data availability statement

All original data reported in this manuscript are available from the corresponding author upon reasonable request.

Competing interests

None declared.

Author contributions

P.G.T. performed surgical work and *in situ* measurements, data analyses and drafted the manuscript. P.W.H. completed histological staining, image analysis and drafted the manuscript. A.W. programmed the LabVIEW software. M.H.N. assisted with wheel-running experiments. H.D. and S.E. conceived the research, assisted with experimental work, data analysis and drafting the manuscript. All authors approved the final version.

Funding

This research was funded by a British Heart Foundation Project Grant (PG/14/15/30691).

Acknowledgements

We thank Roger Kissane for assistance with PO_2 modelling.

Keywords

blood flow, cardiac hypertrophy, fatigue, microcirculation, skeletal muscle

Supporting information

Additional supporting information can be found online in the Supporting Information section at the end of the HTML view of the article. Supporting information files available:

Peer Review History
Statistical Summary Document

Translational Perspective

Poor skeletal muscle function is thought to contribute to exercise intolerance in diseases such as chronic heart failure. Tiny blood vessels are normally intertwined with muscle fibres to deliver oxygen and nutrients. However, these capillaries become less abundant with the onset of disease, potentially causing a limitation on how well the muscle can function. In this paper, we tested whether incipient heart disease (surgically induced by hypertension-linked compensatory cardiac enlargement) in a rat model results in loss of blood-perfused capillaries and muscle function, and whether aerobic exercise or muscle stretch are effective therapeutic treatments for this impairment. Critically, loss of functional capillaries occurred alongside the onset of disease, and this coincided with the muscle being prone to rapid fatigue. Despite the development of incipient heart disease, aerobic exercise and muscle stretch independently normalized these pathological changes, resulting in muscle fatigue that was indistinguishable from control values. This functional improvement after intervention corresponded to an enhanced supply of perfused capillaries, which improved the oxygen supply to exercising muscle tissue. These results highlight the efficacy of targeting the muscle capillaries for restoration of muscle performance, and underscore the importance of this therapeutic target for alleviating the symptoms of exercise intolerance in clinical disease.